ACS OMEGA

Open Access

http://pubs.acs.org/journal/acsodf

Article

Fluorination Modification of Methyl Vinyl Silicone Rubber and Its Compatibilization Effect on Fluorine/Silicone Rubber Composites

Shuwen Xing, Chuhui Yu, Lei Ding, Shuaiqi Li, Gao Pan, Mengyu Jin, Li Liu,* and Shipeng Wen*

Cite This: *ACS Omega* 2024, 9, 20388−20396

Read Online

ACCESS | Metrics & More | Article Recommendations | Supporting Information

ABSTRACT: Among numerous rubbers, high-performance rubber composites can be obtained by mixing fluororubber (FKM) with excellent oil resistance and silicone rubber (SiR) with excellent low-temperature resistance. While the difference in polarity between these two kinds of rubbers leads to a reduction in the properties of the composites. To solve the compatibility problem between the two-phase interfaces in FKM/SiR composites, in this research, fluorinated silicone rubbers (MVQ-*g*-PFDT) of methyl vinyl silicone rubber (MVQ) grafted with 1H,1H,2H,2H-perfluorodecanethiol (PFDT) were prepared via a facile and efficient thiol−ene click reaction, which was then added into FKM/SiR composites. The results showed that the fluorine-containing side chains could effectively inhibit the low-temperature crystallization phenomenon of silicone rubber and further broaden its application ranges in low-temperature environments. The properties of FKM/SiR composites with the addition of MVQ-*g*-PFDT were significantly improved, with the highest tensile strength of 14.1 MPa and the lowest mass change rate of 6.71% after 48h immersion at 200 °C in IRM903 oil. Additionally, the hydroxyl groups between the fluorine-containing side chains of MVQ-*g*-PFDT and the surface of silica facilitate the enhancement of the uniform dispersion of fillers. Atomic force microscopy (AFM) characterization results showed a distinct enhancement of the compatibility between the two phases of FKM and SiR. This work would provide further insight into efforts to improve compatibility between rubbers with widely different polarities.

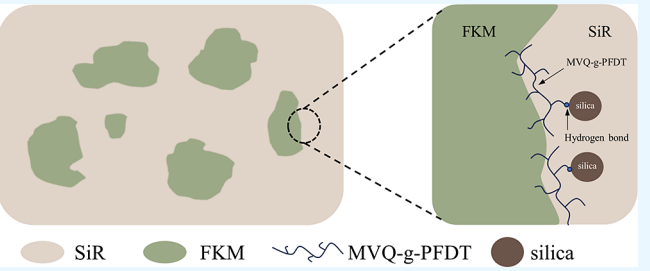

1. INTRODUCTION

MVQ main chain consists of alternating Si and O atoms with good flexibility, and its special molecular structure gives it the widest application temperature range among synthetic rubbers.[1,2] However, the methyl and vinyl groups in the side chain of MVQ are nonpolar groups,[3] which make it less resistant to nonpolar oils.[4,5] Additionally, the regular molecular chain structure of MVQ can lead to crystallization at low temperatures,[6] which narrows its range of application. Therefore, polar functionalization modification of MVQ is essential. Thiol−ene click chemistry is a green and efficient molecular structure design reaction, commonly used in the molecular chain functionalization modification of polymers.[7,8] In the functionalization modification of silicone elastomers, this reaction is commonly used to enhance the polarity by grafting polar groups such as carboxyl,[9] hydroxyl,[10] and epoxy[11] groups onto the side chain of the siloxane. PFDT, a sulfhydryl reagent containing a large number of F elements and has an excellent reactivity, can be grafted onto the surface of MVQ as a reaction substrate, which thereby endowed it with certain antifouling and self-repairing ability.[12−14]

Silicone rubber is soft and elastic, but its physical and mechanical properties are poor.[15] Therefore, when it is in application, other specialty rubbers, such as ethylene propylene trioxide (EPDM),[16,17] ethylene vinyl acetate (EVA),[18] and FKM,[19] are usually blended to enhance its performance. Among them, the F atom in FKM with a relatively small radius can be closely arranged around the carbon atom and form a protective barrier for the C−C bond due to the strong electron-absorbing effect of the F atom. The narrowed length and increase in bond energy of the C−C bond would confer the fluorine-containing polymer elastomers with chemical inertia of the carbon chain, heat resistance, oxidation resistance, oil resistance, and other properties.[20−24] After blending with silicone rubber, the fluorine/silicone rubber composite material combines the advantages of silicone rubber and fluorine rubber, with good resistance to high and low temperatures and oil resistance,[25,26] while reducing the cost of use. However, because of the large difference in polarity between these two kinds of rubbers, the compatibility of fluorine/silicone phases is poor, which affects the blending effect and performance.[27,28] The addition of a third component compatibilizer might be a simple and effective way to achieve a more homogeneous fluorine/silicon blend system. Khanra and

Received: January 28, 2024
Revised: April 12, 2024
Accepted: April 16, 2024
Published: April 24, 2024

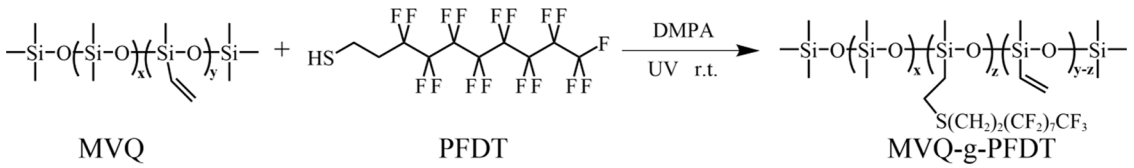

Figure 1. Synthesis reaction of MVQ-*g*-PFDT.

colleagues[29−32] prepared MVQ-*g*-maleic anhydride and FKM-*g*-acrylamide by melt grafting process, and successfully improved the compatibility after adding them into FKM/MVQ blends, which showed improvement in mechanical properties, thermal stability, and aging properties. In addition, the synergistic effect of fluorosilicone rubber with silica and the reaction of glutaraldehyde (GA) with silanol groups on the surface of silica dispersed in different phases to improve the compatibility of FKM/MVQ blends are also reported. Guo et al.[33,34] prepared MVQ-*g*-2,2,2-trifluoroethyl methacrylate and FKM-*g*-vinyl thiethoxysilane as effective compatibilizer in FKM/MVQ blends. The optimal addition of MVQ-*g*-2,2,2-trifluoroethyl methacrylate was 6 phr, and the optimal addition of FKM-*g*-vinyl thiethoxysilane was 9 phr, and the thermal aging properties and low-temperature properties of the composites were improved.

In this work, MVQ-*g*-PFDT was prepared by a simple and fast thiol−ene click chemistry grafting method. It not only successfully suppressed the low-temperature crystallization phenomenon of the silicone rubber but also has the potential for application in the oil-resistant scenarios under special working conditions due to its strong polarity. Subsequently, MVQ-*g*-PFDT was added into the FKM/SiR composites as interfacial compatibilizer, which effectively improved the mechanical properties, and hot-air and hot-oil aging resistance of the composites. At the same time, the thickness of the interfacial interface between the two phases was increased.

2. EXPERIMENT

2.1. Materials. The MVQ used for the grafting reaction was prepared in the laboratory, with a vinyl content of about 10 mol % and a molecular weight of about 30 × 10^4. 1H,1H,2H,2H-perfluorodecanethiol (PFDT) and 2,2-bimethoxy-2-phenylacetophenone (DMAP) were purchased from McLean Co., Ltd. Tetrahydrofuran (THF) and anhydrous ethanol were provided by Beijing Chemical Reagent Co., Ltd. Silicone rubber (110−2, vinyl content 0.17 mol %, molecular weight 54 × 10^4) was purchased from Dongjue Co., Ltd. Fluorine rubber (G912, Mooney viscosity 54 (ML (1 + 10) 121 °C) was purchased from Daikin Co., Ltd. Fumed silica (A200) was obtained from Nippon SOL Co., Ltd., and hydroxyl silicone oil (GY209) was purchased from Zhonghao Chenguang Co., Ltd. Di-*tert*-butyl 1,1,4,4-tetramethyltetramethylene diperoxide (DBPMH) was supplied by Shanghai Fangruida Chemicals Co., Ltd., and triallyl isocyanuronate (TAIC) was supplied by Evonik Co., Ltd.

2.2. Synthesis of MVQ-*g*-PFDT. The synthesis reaction of MVQ-*g*-PFDT is shown in Figure 1. First, the MVQ was fully dissolved in tetrahydrofuran (THF, wt % = 10 g/100 mL) and then 1.2 equiv (to vinyl) of the corresponding PFDT were added and stirred for 30 min. Second, 1% equivalents (to vinyl) of the DMPA were added, and the reaction was triggered by irradiation of the mixed solution with a 365 nm wavelength UV-LED (CEM-F61-2030, Cousz Precision Photoelectric Co., Ltd., China) surface light source for 5 min in an airtight chamber. Finally, at the end of the reaction, the product was flocculated with diploid volume of ethanol solution, redissolved in THF, and then flocculated again with ethanol solution, repeated three times, and then dried in a vacuum oven at 55 °C to a constant weight, and the residual solvent was removed to obtain MVQ-*g*-PFDT.

2.3. Preparation of FKM/SiR Composites. The samples of FKM/SiR composites were prepared using uniform mixing technology. First, silicone rubber was added to the two-roll mill (Shanghai Rubber Machinery Works No. 1, Co., Ltd., China) to form a smooth and seamless roll cover layer after adding MVQ-*g*-PFDT, fumed silica, and hydroxyl silicone oil were added, and then mixed uniformly at room temperature to get the silicone rubber composites. Second, fluorine rubber was plasticized on the two-roll mill for 5 min after appropriately adjusting the roller distance to 1 mm, silicone rubber composites were added and mixed uniformly, and finally the vulcanization system was added (DBPMH and TAIC). Table 1 shows formulation details. The optimum curing time (T_{90}) of the blends was measured by disc rheometer (Beijing Huanfeng Chemical Machinery Trial Plant, China) after 12 h of parking, followed by vulcanization in an automatic vulcanizing press (Huzhou Dongfang Machinery Co., Ltd., China) at 165 °C and 15 MPa, with a vulcanization time of T_{90} + 2 min. The second stage of vulcanization was carried out in a blower oven at a temperature of 200 °C and a time of 4 h.

Table 1. Formulations of FKM/SiR Composites[a]

formulation	0	2	4	6	8	10
SiR/g	50	48	46	44	42	40
MVQ-*g*-PFDT/g	0	2	4	6	8	10
FKM/g	50	50	50	50	50	50

[a]Others (g): fumed Silica (20), hydroxyl silicone oil (2.5), DBPMH (1.65), and TAIC (2.15).

2.4. Characterization. Fourier infrared (FT-IR) spectroscopy was tested by an infrared spectrometer (Tensor 27, Bruker (Beijing) Technology Co., Ltd., China), in ATR mode, with a scanning range of 3500−600 cm^{-1}. Hydrogen nuclear magnetic resonance spectroscopy (^{1}H NMR), carbon nuclear magnetic resonance spectroscopy (^{13}C NMR), and silicon nuclear magnetic resonance spectroscopy (^{29}Si NMR) were characterized using a nuclear magnetic resonance spectrometer (AV 600, Bruker (Beijing) Technology Co., Ltd., China), with deuterated chloroform ($CDCl_3$) as the solvent. GPC (1260 Infinity, Agilent (Beijing) Technology Co., Ltd., China) was used to analyze the molecular weight and molecular weight distribution of the rubber. The contact angle of silicone rubber with water and glycol was measured using an optical contact angle meter (OCA20, DATAPHYSICS Co., Ltd., USA), and then the surface energy of the rubber was calculated according to the Owens-Wendt-Rabel-Kaelble (OWRK) method.[35,36] Differential scanning calorimetry (DSC, STARe system, METTLER-TOLEDO Co., Ltd., Switzerland) was used to

https://doi.org/10.1021/acsomega.4c00015
ACS Omega 2024, 9, 20388−20396

determine the glass transition temperature and crystallization temperature of the rubber. The temperature was reduced from 20 to −135 °C in a nitrogen atmosphere at a cooling rate of −10 °C/min and held at −135 °C for 5 min, followed by warming from −135 to 20 °C at a rate of 10 °C/min. Thermal stability was evaluated by a thermogravimetric analyzer (TG, STARe system, METTLER-TOLEDO Co., Ltd., Switzerland). Samples of 10 mg were heated from 30 to 800 °C at a heating rate of 10 °C min^{-1} under nitrogen. The SEM (S4800, Hitachi Co., Ltd., Japan) was used to observe the microstructure of FKM/SiR composites. Vulcanization properties was determined with a rotorless vulcanizer (M-3000A, Gotech Co., Ltd., China) with a shear angle of 5° and a frequency of 200 cpm, including the highest torque (M_H), lowest torque (M_L), incremental torque of the material (M_H−M_L), scorch time (T_{10}), and optimum curing time (T_{90}). Equilibrium dissolution method was used to test the cross-linking density of the samples. The specimen (initial mass m_0) was immersed in toluene for 72 h at room temperature, and its mass m_1 after dissolution was tested immediately after drying the liquid on the surface. Then, the specimen was dried in a blower oven at 70 °C until the mass did not change anymore, its mass m_2 was tested, and its cross-linking density (V_e) was calculated according to the following formula.

$$V_e = -\frac{\ln(1 - V_r) + V_r + \chi V_r^2}{V_s(V_r^{1/3} - \frac{V_r}{2})} \quad (1)$$

where V_r represents the volume fraction, which is calculated by the following equation; χ represents the interaction parameter between the solvent and rubber; and V_s is the molar volume of toluene.

$$V_r = \frac{(m_2 - m_0\varphi)/\rho_r}{(m_2 - m_0\varphi)/\rho_r + (m_1 - m_2)/\rho_s} \quad (2)$$

where φ represents the mass fraction of insoluble components in rubber; ρ_r represents the density of rubber; and ρ_s represents the density of solvent.

The interface of the blends was characterized by atom force microscopy (AFM, Bruker (Beijing) Technology Co., Ltd., China) after freeze-polishing, which was operated at room temperature in PeakForce QNM mode. Tensile properties and tear properties were tested with an electronic tensile tester (CMT4104, Shenzhen SANS Test Machine Co., Ltd., China). Samples were cut into dumbbell-shaped and right-angled test strips with a length of 25 mm and tested at a rate of 500 mm/min. The hardness of the samples was tested at room temperature with a Shore A durometer. The hot-air aging resistance was characterized by placing the dumbbell-shaped and right-angled test strip in a 200 °C blower oven for 48 h and testing the tensile properties, tear properties, and their changes (ΔTensile strength or tear strength).

$$\Delta\text{Tensile strength or tear strength}\ (\%) = \frac{\text{Value before ageing} - \text{Value after ageing}}{\text{Value before ageing}} \times 100\% \quad (3)$$

The samples were cut into 10 mm × 10 mm test strips and placed in IRM903 oil at 200 °C for 48 h, and the mass change rates (Δm) and volume change rates (ΔV) were tested to characterize the hot-oil aging performance.

$$\Delta m\ (\%) = \frac{\text{Final mass} - \text{Initial mass}}{\text{Initial mass}} \times 100\% \quad (4)$$

$$\Delta V(\%) = \frac{\text{Final volumes} - \text{Initial volumes}}{\text{Initial volumes}} \times 100\% \quad (5)$$

3. RESULTS AND DISCUSSION

3.1. Structure and Properties of the MVQ-*g*-PFDT.

Figure 2 shows the comparison of infrared spectra of MVQ and MVQ-*g*-PFDT, and it is evident that after grafting, the original characteristic peaks of silicone rubber, such as the Si−O−Si telescopic vibration peaks at 1015 and 1084 cm^{-1} and the Si−C telescopic vibration peaks at 1412 cm^{-1} were retained. The CF_2 characteristic peaks appeared at 1212 cm^{-1}, which demonstrated that fluorine has been introduced. The appearance of the characteristic C−S−C peak at 1146 cm^{-1} proves that PFDT was successfully grafted onto the silicone rubber side chain.

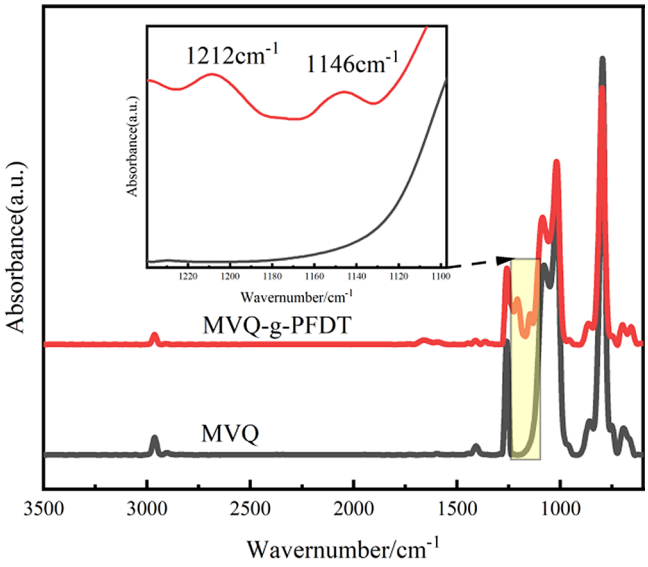

Figure 2. Infrared spectra of MVQ and MVQ-*g*-PFDT.

The chemical structure of MVQ-*g*-PFDT was further demonstrated using ^{1}H NMR, ^{13}C NMR, and ^{29}Si NMR (Figure 3). Two hydrogen chemical shifts on $-CH_2-$ linked to S appeared in the ^{1}H NMR spectrum at δ = 2.61 ppm, δ = 2.72 ppm and respectively corresponded to the two chemical shifts at δ = 22 ppm, δ = 18 ppm in the ^{13}C NMR spectrum, which proved that the reaction of -SH dehydrogenation with $-CH{=}CH_2$ resulted in fluorine-containing small molecules grafted on the side chain of MVQ. Dense peaks appeared between δ = 110 and 120 ppm in ^{13}C NMR, which was due to the powerful electronegativity of F that weakened the shielding effect and shifted the C resonance peaks connected to it to the low field, and the induced effect that made the $-CF_2-$, $-CF_3$ appeared in the low-field intervals. In the ^{29}Si NMR spectrum, a broad peak at δ = −110 ppm for Si attached to the side chain of the PFDT further confirmed the presence of the aforementioned chemical structure.

Figure 4a,b shows the comparison of DSC curves and TGA curves of silicone rubber before and after grafting, respectively, in order to characterize the effect of grafting modification on the low- and high-temperature properties of silicone rubber.

https://doi.org/10.1021/acsomega.4c00015
ACS Omega 2024, 9, 20388−20396

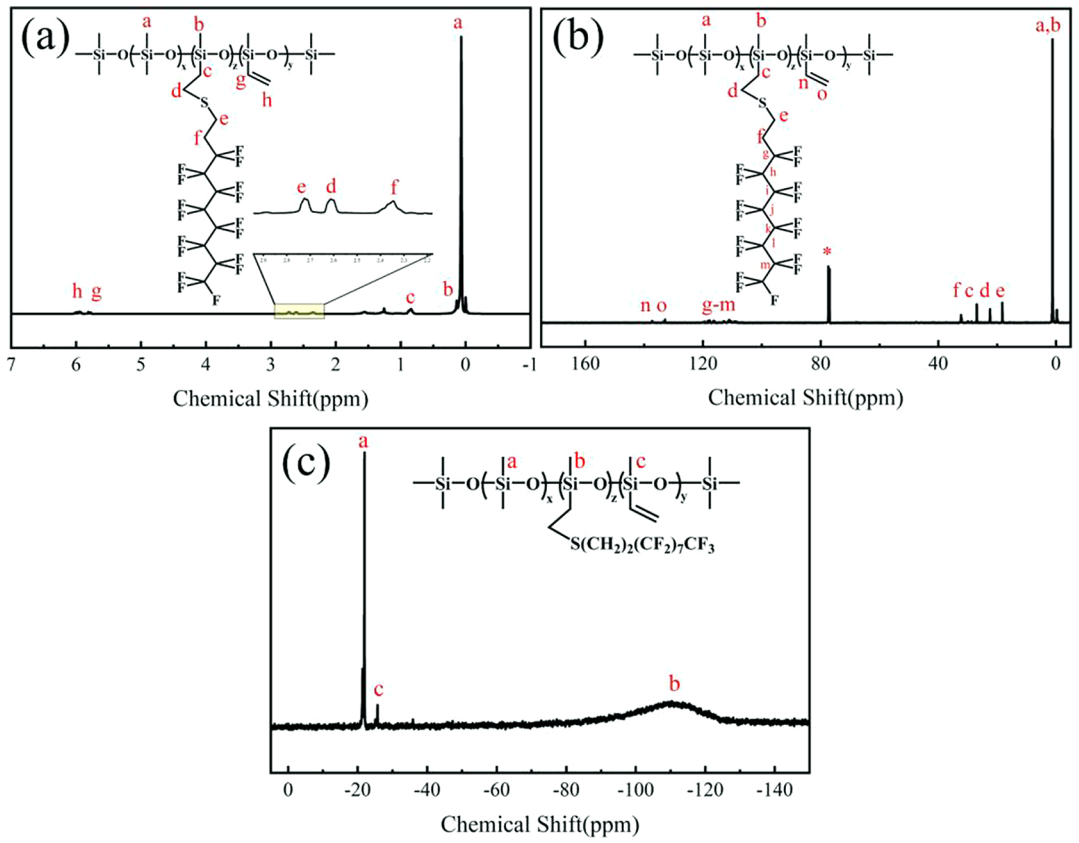

Figure 3. (a) ^{1}H NMR spectrum, (b) ^{13}C NMR spectrum, and (c) ^{29}Si NMR spectrum of MVQ-*g*-PFDT.

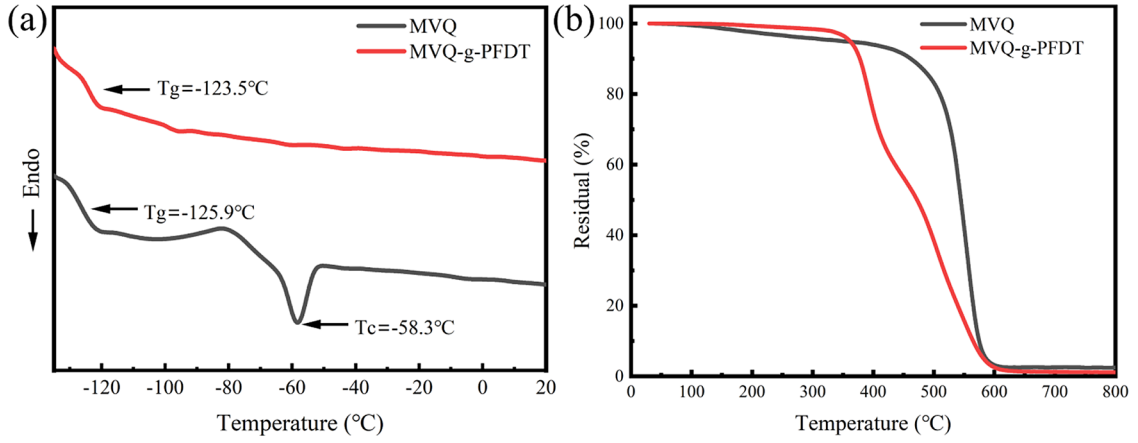

Figure 4. (a) DSC thermograms. (b) TGA thermograms of MVQ and MVQ-*g*-PFDT.

After grafting, T_g increased from −125.9 to −123.5 °C because the fluorine-containing side chains decreased the silicone rubber molecular chain flexibility and increased the difficulties of molecular chain movement leading to the increase of the glass transition temperature. For MVQ, a clear crystallization peak at −58.3 °C had disappeared after grafting. The fluorine-containing side chains disrupted the rubber chain segment regularity, and thus effectively inhibited the phenomenon of silicone rubber crystals at low temperatures (i.e., improved the low-temperature performance). Table 2 shows TGA data of MVQ and MVQ-*g*-PFDT. Different from MVQ, the thermal degradation of MVQ-*g*-PFDT is divided into two stages: at T_{max1} = 394 °C corresponding to the degradation of the fluorinated side chain; and at T_{max2} = 518 °C, corresponding to the cleavage of siloxane bonds, this trend can be observed more visually with DTG images (Figure S1). Through side group oxidation and radical reactivity, vinyl can create an extremely dense networked structure that acts as a barrier

Table 2. TGA Data of MVQ and MVQ-*g*-PFDT[a]

samples	$T_{5\%}$/°C	$T_{50\%}$/°C	T_{max1}/°C	T_{max2}/°C	residual/%
MVQ	348	545	555		2.5
MVQ-*g*-PFDT	365	472	394	518	1.3

[a] $T_{5\%}$: 5% weight loss temperature; $T_{50\%}$: 50% weight loss temperature; T_{max1}: temperature of maximum rate of the first degradation stage; T_{max2}: temperature of maximum rate of the second degradation stage; and residual: char yield at 800 °C.

https://doi.org/10.1021/acsomega.4c00015
ACS Omega 2024, 9, 20388−20396

against heat and oxygen erosion, better safeguarding the internal structure from damage. It can effectively inhibit the degradation of the back bite cyclization of the silicone rubber main chain. Since $-CH{=}CH_2$ is thermally more stable than the fluorinated side chain, the grafted MVQ-*g*-PFDT has a slight decrease in thermal stability and a lower residual carbon rate at 800 °C.

In order to characterize the changes in the polarity of the silicone rubber before and after grafting, contact angle tests were performed on MVQ and MVQ-*g*-PFDT (Figure 5 and

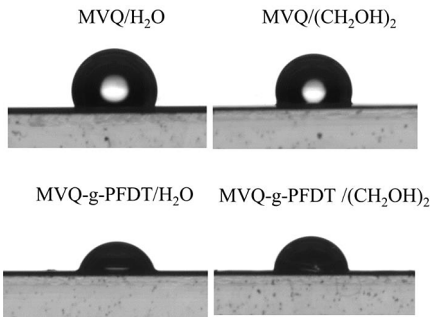

Figure 5. Contact angles of MVQ and MVQ-*g*-PFDT.

Table 3. Contact Angle and Surface Free Energy of MVQ and MVQ-*g*-PFDT

samples	θ/H_2O	$\theta/(CH_2OH)_2$	surface free energy/mN·m^{-1}
MVQ	112.7°	114.75°	8.86
MVQ-*g*-PFDT	75.6°	83.3°	41.37

Table 3). The contact angle of the modified MVQ-*g*-PFDT decreased dramatically with both water and glycol contact angles less than 90°, and the surface energy was substantially improved. The introduction of fluorine-containing side groups has significantly increased the polarity of silicone rubber,[12] which contributes to improve its compatibility with fluorine rubber.

3.2. Microstructure Observation of FKM/SiR Composites. The microscopic observation of the dispersion of silica filler inside the composites was carried out by scanning electron microscopy, and the results are shown in Figure 6. As an important reinforcing filler, the dispersion of silica particles in the rubber matrix will directly affect the mechanical properties of rubber. In Figure 6, the dark part is the rubber matrix and the white irregular particles are silica fillers. It can be clearly observed that with the increase of MVQ-*g*-PFDT addition, the silica distribution is more uniform; under the same magnification, more silica particles appear in the field of view, and the large blank area where silica does not appear is significantly reduced. This phenomenon is mainly attributed to the hydrogen bonding between the silica hydroxyl groups on the surface of silica and the fluorine-containing side groups in MVQ-*g*-PFDT, which results in a more uniform dispersion in the matrix.

3.3. Vulcanization Properties of FKM/SiR Composites. Table 4 shows the vulcanization performance parameters of FKM/SiR composites when MVQ-*g*-PFDT is added in different portions. With the increase of the amount of MVQ-*g*-PFDT from 0 to 10 g, the scorch time (T_{10}) of the rubber composites did not change much and stayed at about 0.5 min; the optimum vulcanization time (T_{90}) increased, because the

Table 4. Vulcanization Characteristic Parameters of Composites with Different MVQ-*g*-PFDT

	MVQ-*g*-PFDT/g					
characteristics	0	2	4	6	8	10
M_L/dN·m	1.98	2.34	2.74	2.33	2.41	2.73
M_H/dN·m	16.39	18.78	19.87	19.08	19.47	20.27
ΔM/dN·m	14.41	16.44	17.13	16.75	17.06	17.54
T_{10}/min	0.49	0.49	0.48	0.50	0.52	0.49
T_{90}/min	3.49	3.16	3.36	3.95	4.80	4.35

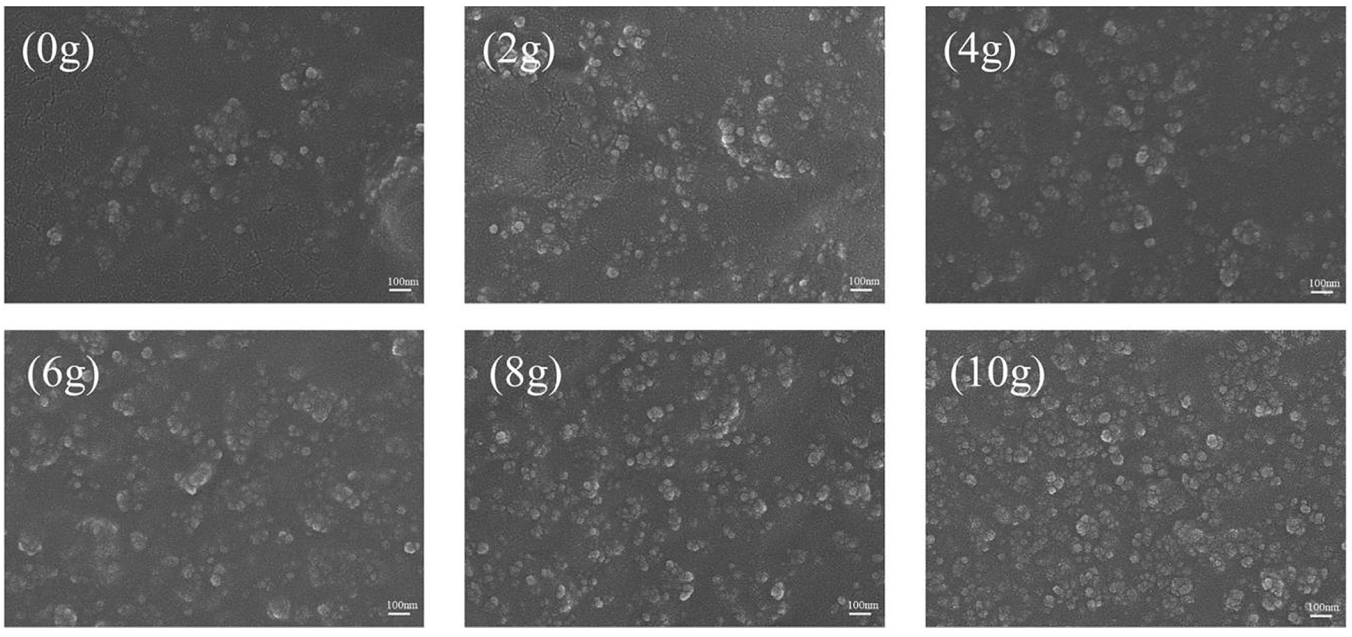

Figure 6. SEM images of composites with different MVQ-*g*-PFDT.

https://doi.org/10.1021/acsomega.4c00015
ACS Omega 2024, 9, 20388−20396

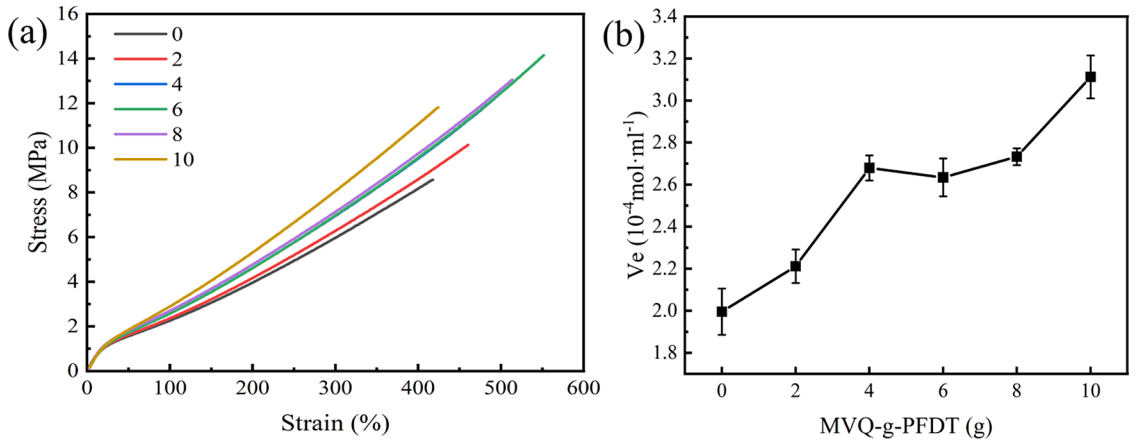

Figure 7. (a) Stress−strain curves of composites with different MVQ-*g*-PFDT. (b) Cross-linking density of composites with different MVQ-*g*-PFDT.

Table 5. Mechanical Property Parameters of Composites with Different MVQ-*g*-PFDT

	MVQ-*g*-PFDT/g					
characteristics	0	2	4	6	8	10
tensile strength/MPa	8.6 ± 0.8	10.1 ± 1.3	12.1 ± 1.6	14.1 ± 0.8	13.0 ± 0.9	11.8 ± 0.6
elongation at break/%	418 ± 38	460 ± 40	492 ± 49	552 ± 26	514 ± 32	424 ± 19
tear strength/kN·m^{-1}	15.0 ± 0.4	16.1 ± 1.9	16.0 ± 1.3	16.8 ± 1.9	14.5 ± 2.1	15.9 ± 1.2
100% modulus/MPa	2.3 ± 0.1	2.4 ± 0.1	2.6 ± 0.1	2.6 ± 0.1	2.7 ± 0.1	2.9 ± 0.1
300% modulus/MPa	6.0 ± 0.1	6.3 ± 0.2	7.0 ± 0.1	7.0 ± 0.1	7.1 ± 0.1	8.1 ± 0.1
shore A hardness	62 ± 1	60 ± 1	65 ± 1	66 ± 1	64 ± 1	68 ± 1

thermal decomposition of MVQ-*g*-PFDT produced a proportion of the HF, and then the excessive acidity inactivated part of the peroxide vulcanizing agent, further slowing down the vulcanization rate. Both the maximum torque (M_H) and torque difference (ΔM) increased due to the enhanced combination of silicone/fluorine two-phase, prompting the rubber to form a dense cross-linking network.

3.4. Mechanical Properties of FKM/SiR Composites. The static mechanical properties of the FKM/SiR composites were tested after the addition of the MVQ-*g*-PFDT, stress−strain curves are shown in Figure 7a and the performance parameters are shown in Table 5. The tensile strength, tear strength, and elongation at break showed approximate trends, and the mechanical properties first increased and then decreased with the increase of the number of added portions of MVQ-*g*-PFDT, reaching the maximum at the same time with the addition of 6 g MVQ-*g*-PFDT. In the grafting reaction process of MVQ-*g*-PFDT, there were molecular chain breakage, cyclic degradation, and other side reactions; the GPC data (Table S1) shows a decrease in molecular weight from 30.7 × 10^4 to 24.1 × 10^4 and a broadening of the distribution. So the performance of FKM/SiR composites was inferior when the amount of additive was more than 6 g. The increase in hardness and 300% modulus was attributed to the increase in cross-link density within the rubber, which was consistent with the conclusions drawn from Figure 7b.

The internal cross-linking density of FKM/SiR composites was determined, and the results are shown in Figure 7b. SiR framed the cross-linked network through the initiation of vinyl groups in the side chains by the peroxide vulcanizing agent; and the MVQ-*g*-PFDT contained vinyl groups itself and therefore was added to the cross-linked network. As the number of added portions of MVQ-*g*-PFDT increased, the cross-link density increased, which was in line with the results of cross-link density changes predicted by the trends of M_H and ΔM parameters in the vulcanization performance. There are two main reasons for this phenomenon: (i) MVQ-*g*-PFDT induces an enhanced interaction between the two interfaces of FKM and SiR, which can be proven by the AFM characterization (Figure 8); (ii) the formation of hydrogen bonding between MVQ-*g*-PFDT and the silica hydroxyl groups on the surface of silica creates additional cross-linking points, which is the reason for a more homogeneous distribution of silica in the rubber matrix, which can be clearly observed in the SEM image (Figure 6).

3.5. Compatibility Characterization of FKM/SiR Composites. The dispersion of fluorine rubber in the composites was qualitatively observed by AFM, and the thickness of the phase interface between the two phases of FKM and SiR was further quantitatively characterized (Figures 8 and S2). The darker areas correspond to higher modulus FKM, and the lighter areas correspond to lower modulus SiR[37] in Figure 8a,c and a1,c1. As the addition fraction of MVQ-*g*-PFDT is increased from 0 to 10 g, FKM is more homogeneously distributed in the SiR with a smaller particle size. Modulus versus phase interface size images (Figure 8a2,c2) were obtained by sampling calculation of Figure 8a1,c1. The thickness of the two-phase interface was obviously increased from 103.19 to 234.38 nm, and the compatibility is significantly improved.

3.6. Aging Resistance of FKM/SiR Composites. The mechanical properties of FKM/SiR composites were measured after aging in hot-air at 200 °C for 48h (Figure 9a). The trend of mechanical properties after aging did not change: it still increased and then decreased with the increase of the amount of additive, and the tensile strength and tear strength reached

https://doi.org/10.1021/acsomega.4c00015
ACS Omega 2024, 9, 20388−20396

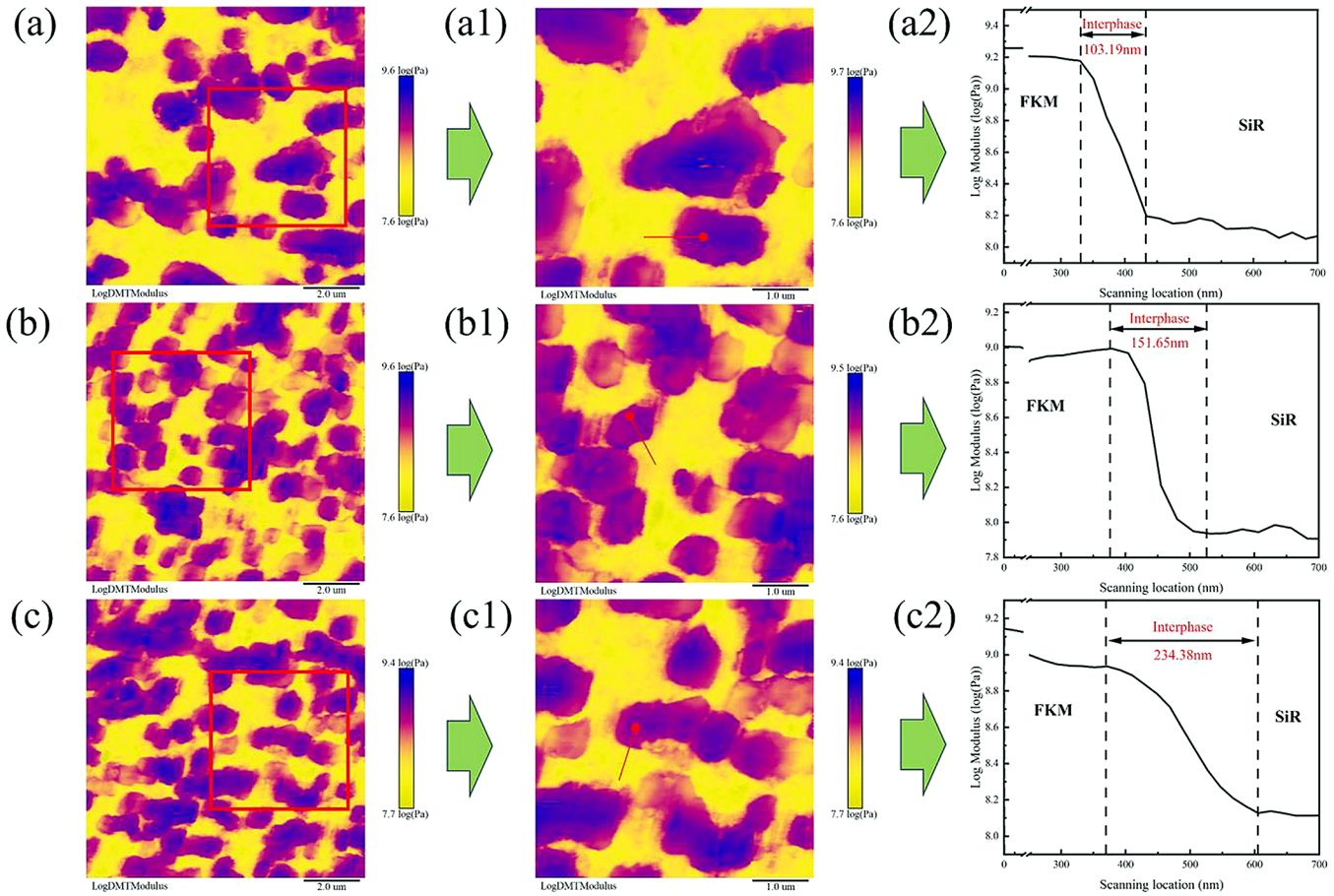

Figure 8. AFM modulus images (a, c), after 2× magnification images (a1, c1), and corresponding log modulus curve (a2, c2) of composites with 0, 6, and 10g MVQ-*g*-PFDT additions.

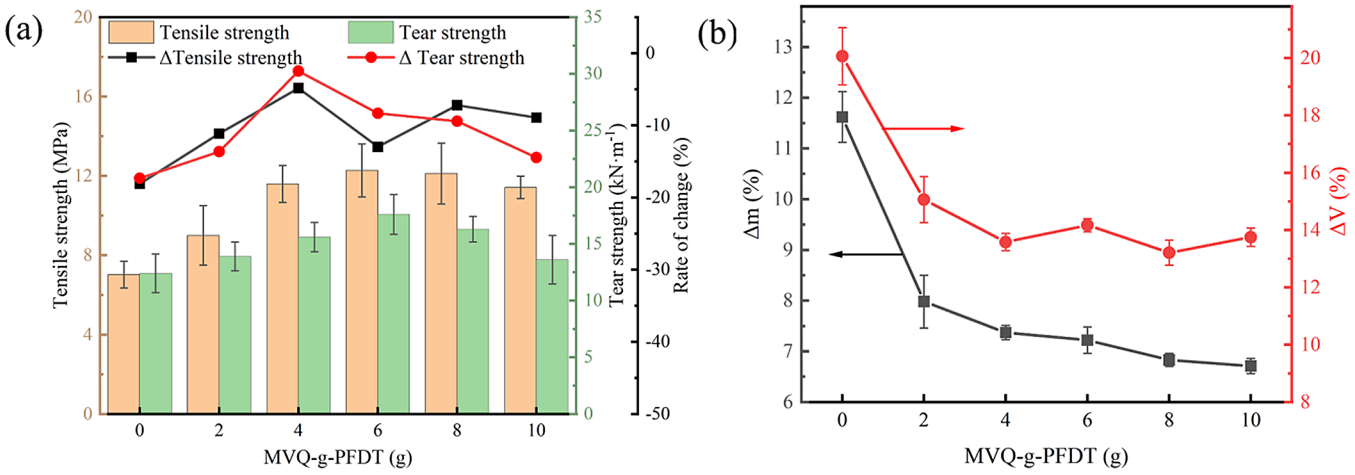

Figure 9. (a) Hot-air aging resistance of composites with different MVQ-*g*-PFDT. (b) Hot-oil aging resistance of composites with different MVQ-*g*-PFDT.

the maximum value when 6 g MVQ-*g*-PFDT were added. When the addition amount is 4 g, the rates of change in tensile strength and tear strength before and after aging reached the lowest, and the hot-air aging resistance was optimal. The addition of MVQ-*g*-PFDT effectively enhanced the thickness of the interface between the two phases of silicone/fluorine so that the shielding effect of fluorine rubber on the molecular chain of silicone rubber was enhanced with better heat resistance, thus improving the hot-air aging resistance of the composite.

Volume expansion and mass change of rubber materials caused by long-term immersion in hot-oil are substantial factors limiting the application of rubber. The hot-oil resistance of the composites was characterized by testing the rate of mass change and volume change after 48 h of immersion at 200 °C in IRM 903, and the results are shown in Figure 9b. The results

https://doi.org/10.1021/acsomega.4c00015
ACS Omega 2024, 9, 20388−20396

showed that the addition of MVQ-*g*-PFDT resulted in a significant increase in the oil resistance of the composites: the rate of change in mass reached a minimum of 6.83% with the addition of 10 g, which was a 42.25% decrease compared to the unadded sample; and the rate of change in volume reached a minimum of 13.21% with the addition of 8 g, which was 34.15% lower than that of the unadded sample. MVQ-*g*-PFDT improves the dispersion of FKM in SiR, which has better oil resistance and therefore protects the SiR with poor oil resistance. The introduction of fluorine-containing side chains also efficiently improves the polarity of the composite and the migration of internal fillers caused by nonpolar oil swelling.

4. CONCLUSIONS

In this study, MVQ-*g*-PFDT was prepared by thiol−ene click chemistry. The characterization results showed that the polarity increased remarkably, and the low-temperature crystallization was inhibited. Also, the low-temperature properties of methyl vinyl silicone rubber were effectively improved. By addition of MVQ-*g*-PFDT into FKM/SiR composites, the interfacial thickness between the two phases of FKM and SiR increased, and the compatibility enhancement led to a significant improvement in the mechanical properties of the composites, hot-air aging resistance, and hot-oil aging resistance. By improving the compatibility of FKM/SiR composites, it is expected that the substitution of fluorosilicone rubber and cost reduction can be accomplished.

■ ASSOCIATED CONTENT

Supporting Information

The Supporting Information is available free of charge at https://pubs.acs.org/doi/10.1021/acsomega.4c00015.

DTG thermograms of MVQ and MVQ-*g*-PFDT; GPC data of MVQ and MVQ-*g*-PFDT; and AFM modulus images of composites with different MVQ-*g*-PFDT (PDF)

■ AUTHOR INFORMATION

Corresponding Authors

Li Liu − *State Key Laboratory of Organic−Inorganic Composites, Beijing University of Chemical Technology, Beijing 100029, PR China; Engineering Research Center of Elastomer Materials on Energy Conservation and Resources, Ministry of Education, Beijing 100029, PR China*; Email: liul@mail.buct.edu.cn

Shipeng Wen − *State Key Laboratory of Organic−Inorganic Composites, Beijing University of Chemical Technology, Beijing 100029, PR China; Engineering Research Center of Elastomer Materials on Energy Conservation and Resources, Ministry of Education, Beijing 100029, PR China*; orcid.org/0000-0001-9540-1314; Email: wensp@mail.buct.edu.cn

Authors

Shuwen Xing − *State Key Laboratory of Organic−Inorganic Composites, Beijing University of Chemical Technology, Beijing 100029, PR China; Engineering Research Center of Elastomer Materials on Energy Conservation and Resources, Ministry of Education, Beijing 100029, PR China*; orcid.org/0009-0004-8531-104X

Chuhui Yu − *State Key Laboratory of Organic−Inorganic Composites, Beijing University of Chemical Technology, Beijing 100029, PR China; Engineering Research Center of Elastomer Materials on Energy Conservation and Resources, Ministry of Education, Beijing 100029, PR China*

Lei Ding − *China State Shipbuilding Corporation Systems Engineering Research Institute, Beijing 100094, PR China*

Shuaiqi Li − *State Key Laboratory of Organic−Inorganic Composites, Beijing University of Chemical Technology, Beijing 100029, PR China; Engineering Research Center of Elastomer Materials on Energy Conservation and Resources, Ministry of Education, Beijing 100029, PR China*

Gao Pan − *State Key Laboratory of Organic−Inorganic Composites, Beijing University of Chemical Technology, Beijing 100029, PR China; Engineering Research Center of Elastomer Materials on Energy Conservation and Resources, Ministry of Education, Beijing 100029, PR China*

Mengyu Jin − *State Key Laboratory of Organic−Inorganic Composites, Beijing University of Chemical Technology, Beijing 100029, PR China; Engineering Research Center of Elastomer Materials on Energy Conservation and Resources, Ministry of Education, Beijing 100029, PR China*

Complete contact information is available at: https://pubs.acs.org/10.1021/acsomega.4c00015

Notes

The authors declare no competing financial interest.

■ ACKNOWLEDGMENTS

This work was supported by the National Natural Science Foundation of China (Grant No. ZK20180109).

■ REFERENCES

(1) Zang, C. G.; Pan, H. W.; Chen, Y. J. Synergistic Effects between Multiphase Thermal Insulation Functional Phases on the Mechanical and Heat Insulation Properties of Silicone Rubber Composites. *ACS Omega* **2023**, *8* (31), 28026−28035.

(2) Shit, S. C.; Shah, P. A Review on Silicone Rubber. *Natl. Acad. Sci. Lett.-India* **2013**, *36* (4), 355−365. Review. DOI:

(3) Ma, J.; Ma, T.; Duan, W.; Wang, W.; Cheng, J.; Zhang, J. Superhydrophobic, multi-responsive and flexible bottlebrush-network-based form-stable phase change materials for thermal energy storage and sprayable coatings. *Journal of Materials Chemistry A* **2020**, *8* (42), 22315−22326.

(4) Patil, A. O.; Coolbaugh, T. S. Elastomers: A literature review with emphasis on oil resistance. *Rubber Chem. Technol.* **2005**, *78* (3), 516−535. Review. DOI:

(5) Akhlaghi, S.; Gedde, U. W.; Hedenqvist, M. S.; Braña, M. T. C.; Bellander, M. Deterioration of automotive rubbers in liquid biofuels: A review. *Renew. Sust. Energy Rev.* **2015**, *43*, 1238−1248. Review. DOI:

(6) Shi, J.; Zhao, N.; Yan, D.; Song, J.; Fu, W.; Li, Z. Design of a mechanically strong and highly stretchable thermoplastic silicone elastomer based on coulombic interactions. *Journal of Materials Chemistry A* **2020**, *8* (12), 5943−5951.

(7) Lowe, A. B. Thiol−ene "click" reactions and recent applications in polymer and materials synthesis: a first update. *Polym. Chem.* **2014**, *5* (17), 4820−4870.

(8) Hoyle, C. E.; Bowman, C. N. Thiol-Ene Click Chemistry. *Angew. Chem.-Int. Ed.* **2010**, *49* (9), 1540−1573. Review. DOI:

(9) Liu, X.; Sun, H.; Liu, S.; Jiang, Y.; Yu, B.; Ning, N.; Tian, M.; Zhang, L. Mechanical, dielectric and actuated properties of carboxyl grafted silicone elastomer composites containing epoxy-functionalized TiO2 filler. *Chemical Engineering Journal* **2020**, *393*, No. 124791.

(10) Sun, H.; Liu, X.; Yan, H.; Feng, Z.; Yu, B.; Ning, N.; Tian, M.; Zhang, L. The role of dipole structure and their interaction on the

electromechanical and actuation performance of homogeneous silicone dielectric elastomers. *Polymer* **2019**, *165*, 1−10.
(11) Zhang, W.; Hu, S.; Li, H.; Song, T.; Jiang, L.; Zhang, Q.; Zhang, S.; Lu, Y.; Zhang, L. Epoxidized vinyl silicone rubber-based flexible ablative material with low linear ablation rate. *Composites. Communications* **2023**, *40*, No. 101606.
(12) Zhang, X.; Gao, P.; Hollimon, V.; Brodus, D.; Johnson, A.; Hu, H. Surface thiolation of silicon for antifouling application. *Chemistry Central Journal* **2018**, *12* (1), 10.
(13) Xu, F.; Li, X.; Weng, D.; Li, Y.; Sun, J. Transparent antismudge coatings with thermally assisted healing ability. *Journal of Materials Chemistry A* **2019**, *7* (6), 2812−2820.
(14) Zeng, T.; Zhang, P.; Li, X.; Yin, Y.; Chen, K.; Wang, C. Facile fabrication of durable superhydrophobic and oleophobic surface on cellulose substrate via thiol-ene click modification. *Appl. Surf. Sci.* **2019**, *493*, 1004−1012.
(15) Madsen, F. B.; Daugaard, A. E.; Hvilsted, S.; Skov, A. L. The Current State of Silicone-Based Dielectric Elastomer Transducers. *Macromol. Rapid Commun.* **2016**, *37* (5), 378−413.
(16) Qi, S.; Yu, M.; Fu, J.; Zhu, M.; Xie, Y.; Li, W. An EPDM/MVQ polymer blend based magnetorheological elastomer with good thermostability and mechanical performance. *Soft Matter* **2018**, *14* (42), 8521−8528.
(17) Zhang, W. J.; Yan, W.; Pan, R. J.; Guo, W. H.; Wu, G. H. Synthesis of silane-grafted ethylene vinyl acetate copolymer and its application to compatibilize the blend of ethylene-propylene-diene copolymer and silicone rubber. *Polym. Eng. Sci.* **2018**, *58* (5), 719−728.
(18) Ganesh, B.; Unnikrishnan, G. Cure characteristics, morphology, mechanical properties, and aging characteristics of silicone rubber/ethylene vinyl acetate blends. *J. Appl. Polym. Sci.* **2006**, *99* (3), 1069−1082.
(19) Wu, W.; Wang, Y. Vulcanization and Thermal Properties of Silicone Rubber/Fluorine Rubber Blends. *Journal of Macromolecular Science, Part B* **2019**, *58* (6), 579−591.
(20) Xu, Z.; Zhang, Y.; Li, A.; Wang, J.; Wang, G.; He, Q. Research progress on compounding agent and mechanical test method of fluororubber. *J. Appl. Polym. Sci.* **2021**, *138* (4), 50913.
(21) Simon, A.; Pepin, J.; Berthier, D.; Méo, S. Degradation mechanism of FKM during thermo-oxidative aging from mechanical and network structure correlations. *Polym. Degrad. Stab.* **2023**, *208*, No. 110271.
(22) Wu, W.; Jin, B.; Xu, H.; Wu, H.; Yuan, Z.; Xie, Z.; Wen, Y.; Wang, K.; Wu, J. Low-fuel-permeation thermoplastic vulcanizates prepared from mutually miscible fluoroelastomer and poly(vinylidene fluoride−hexafluoropropylene). *Polym. Int.* **2023**, *72* (9), 822−831.
(23) Wang, S.; Wang, C.; He, A. Insights into the effects of high-temperature lubricating oils on the aging behavior and degradation mechanism of fluoroelastomers. *Polym. Eng. Sci.* **2023**, *63* (8), 2371−2384.
(24) Ameduri, B.; Boutevin, B. Update on fluoroelastomers: from perfluoroelastomers to fluorosilicones and fluorophosphazenes. *J. Fluorine Chem.* **2005**, *126* (2), 221−229.
(25) Zhao, X. Y.; Zhang, X. Y.; Li, K. High pressure sealing characteristics of combined structure based on flexible graphite rings. *Adv. Mech. Eng.* **2023**, *15* (6), No. 16878132231182368, DOI: 10.1177/16878132231182368.
(26) Guo, J.; Zeng, X.; Li, H.; Luo, Q. Effect of curatives and fillers on vulcanization, mechanical, heat aging, and dynamic properties of silicone rubber and fluororubber blends. *Journal of Elastomers & Plastics* **2012**, *44* (2), 145−164.
(27) Xu, C.; Wang, Y.; Lin, B.; Liang, X.; Chen, Y. Thermoplastic vulcanizate based on poly(vinylidene fluoride) and methyl vinyl silicone rubber by using fluorosilicone rubber as interfacial compatibilizer. *Materials & Design* **2015**, *88*, 170−176.
(28) Jiang, X.; Chen, K.; Ding, J.; Chen, Y. Structure and Properties of Dynamically Cured Thermoplastic Vulcanizate Based on Poly-(vinylidene fluoride), Silicone Rubber, and Fluororubber. *Polym.-Plast. Technol. Eng.* **2015**, *54* (2), 209−217.
(29) Khanra, S.; Kumar, A.; Ganguly, D.; Ghorai, S. K.; Chattopadhyay, S. The efficacy of methyl vinyl silicone-g-maleic anhydride in the compatibilization of fluoroelastomer and silicone based super specialty elastomer blend. *J. Polym. Res.* **2022**, *29* (5), 174 DOI: 10.1007/s10965-022-03006-5.
(30) Khanra, S.; Kumar, A.; Ganguly, D.; Ghorai, S. K.; Chattopadhyay, S. Effect of FKM-g-acrylamidereactive compatibilizer on mechanical, thermal and aging behaviors of fluoroelastomer (FKM)/silicone rubber (MVQ) blend. *Polym. Eng. Sci.* **2022**, *62* (4), 1239−1255.
(31) Khanra, S.; Ganguly, D.; Ghorai, S. K.; Goswami, D.; Chattopadhyay, S. The synergistic effect of fluorosilicone and silica towards the compatibilization of silicone rubber and fluoroelastomer based high performance blend. *Journal of Polymer Research* **2020**, *27* (4), 96.
(32) Khanra, S.; Sreenivasan, P.; Das, S.; Hore, R.; Ganguly, D.; Chattopadhyay, S. Immobilization of a biobased process aid at the interface for binary silicone and fluoroelastomer based super specialty blends with silica for enhanced compatibility. *J. Mater. Sci.* **2022**, *57* (29), 13974−13990.
(33) Guo, J.; Zeng, X.; Li, H.; Luo, Q. Role of vinyl thiethoxy silane grafted onto fluororubber in compatibilization of fluororubber and silicone rubber blends. *Journal of Elastomers & Plastics* **2013**, *45* (3), 271−288.
(34) Jianhua, G.; Xingrong, Z.; Hongqiang, L.; Quankun, L. Compatibilization of Fluororubber/ Silicone Rubber Blends by the Incorporation of 2,2,2-Trifluoroethyl Methacrylate Grafted Silicone Rubber. *J. Elastomers Plast.* **2010**, *42* (6), 539−560.
(35) Owens, D. K.; Wendt, R. C. Estimation of the surface free energy of polymers. *J. Appl. Polym. Sci.* **1969**, *13*, 1741−1747.
(36) Kaelble, D. H. Dispersion-Polar Surface Tension Properties of Organic Solids. *J. Adhes.* **1970**, *2* (2), 66−81.
(37) Hu, J.; Hao, X.; Ning, N.; Yu, B.; Tian, M. Reactive Janus Particle Compatibilizer with Adjustable Structure and Optimal Interface Location for Compatibilization of Highly Immiscible Polymer Blends. *ACS Appl. Mater. Interfaces* **2023**, *15* (19), 23963−23970.

https://doi.org/10.1021/acsomega.4c00015
ACS Omega 2024, 9, 20388−20396